33rd Annual International Conference of the IEEE EMBS
Boston, Massachusetts USA, August 30 - September 3, 2011

Carotid automated ultrasound double line extraction system (CADLES) via Edge-Flow

Kristen M. Meiburger[1], *Graduate Student Member, IEEE*, Filippo Molinari[1], *Member, IEEE*, Guang Zeng[2], Luca Saba[3], and Jasjit S. Suri[4], *Fellow AIMBE, Senior Member, IEEE*

***Abstract*— This paper presents a completely user-independent algorithm, that automatically extracts the far (distal) double line (lumen-intima and media-adventitia) in the carotid artery using an Edge Flow technique (a class of AtheroEdge™ systems) based on directional probability maps using the attributes of intensity and texture. The extracted double line translates into a measure of the intima-media thickness (IMT), a validated marker for the progression of atherosclerosis. The Carotid Automated Double Line Extraction System based on Edge-Flow (CADLES-EF) is characterized and validated by comparing the output of the algorithm with two other completely automatic techniques (CALEXia and CULEXsa) published by the same authors. Validation was performed on a multi-institutional database of 300 longitudinal B-mode carotid images with normal and pathologic arteries. CADLES-EF showed an intima-media thickness (IMT) bias of 0.043±0.097 mm in comparison to CALEXia and CULEXsa that showed 0.134±0.0.88 mm and 0.74±0.092 mm, respectively. The system's Figure of Merit (FoM) showed an improvement when compared to previous automated methods: CALEXia and CULEXsa, leading to values of 84.7%, 91.5%, while our new approach, CADLES-EF performed the best with 94.8%.**

I. Introduction

The intima-media thickness (IMT) is the most used and validated marker of progression of carotid artery diseases. This can be measured using image processing strategies and *ad-hoc* computer techniques. The goal is to first segment the carotid artery distal wall, so as to then find the lumen-intima (LI) and media-adventitia (MA) boundaries. The distance estimated between these two interfaces is the IMT. The segmentation process can conceptually by thought of as two cascading stages [1]:

- Stage I: recognition of the carotid artery (CA) and delineation of the far adventitia layer (AD_F) in the two-dimensional B-mode ultrasound image;
- Stage II: tracing of the LI/MA wall boundaries in the ROI of the recognized CA. These two stages cannot be independent from each other.

The majority of the algorithms proposed in literature for the automated segmentation of the CA in ultrasound images require a certain degree of user-interaction, which precludes real complete automation. Some recent completely automated techniques that have been developed are based on sustain-attack filters and multi-scale barycenter filters [2], on the use of a Hough transform [3] and on combining dynamic programming and cubic spline [4]. However, all these automated techniques were tested on relatively small datasets acquired by a single sonographer and by the same ultrasound scanner. Since in a real clinical application various aspects can introduce variability (i.e., noise, scanner gain settings, carotid morphology, the presence of normal and pathologic vessels), it is important to test automatic techniques on databases that are multi-institutional, multi-ethnic, and multi-operator.

This paper presents a completely user-independent Carotid Automated Double Line Extraction System using Edge Flow (CADLES-EF) algorithm, which performs both Stages I and II. Starting from the ultrasound image, the algorithm first segments the distal border of the CA and then performs the automatic detection of the LI and MA interfaces. Neither of these processes requires any user interaction. The first part of our new algorithm is based on scale-space multi-resolution analysis while the second part is based on flow field propagation.

II. Architecture of CADLES-EF

CADLES architecture uses a combination of multiresolution and Edge-Flow for our smart automated protocol. AD_F tracing adapts multiresolution scale space-based approach, while LI and MA border segmentation uses Edge-Flow model. Strong LI and strong MA edges are first detected and then refined to yield final LI and MA contours. Combining both strategies, distal (far) double lines (LI and MA) are extraction and IMT estimated.

A. Stage-I: Far Adventitia Tracing

Starting from the automatically cropped image (Figure 1.A), the automated Stage-I is composed of the following stages:

- *Step 1: Fine to Coarse Down-sampling*. The image is first down-sampled by a factor of two (Figure 1.B) adopting a bi-cubic interpolation.
- *Step 2: Speckle reduction*. Speckle noise is attenuated using a first-order local statistics filter (called *lsmv* by the authors [5]), which has given the best performance in the

F. Molinari is with the BioLab, Department of Electronics, Politecnico di Torino, Torino, Italy (Corresponding Author; phone: +39-11-564-4135; fax: +39-11-564-4217; e-mail: filippo.molinari@polito.it).

K.M. Meiburger is with the BioLab, Department of Electronics, Politecnico di Torino, Torino, Italy.

G. Zeng is with the Mayo Clinic, Rochester, MN, USA (gzeng@clemson.edu).

L. Saba is with the Department of Radiology, Azienda Ospedaliero Universitaria di Cagliari, Cagliari, Italy.

J.S. Suri the Biomedical Technologies Inc., Denver, CO, USA and (Aff.) Idaho State University, Pocatello, ID, USA (jsuri@comcast.net).

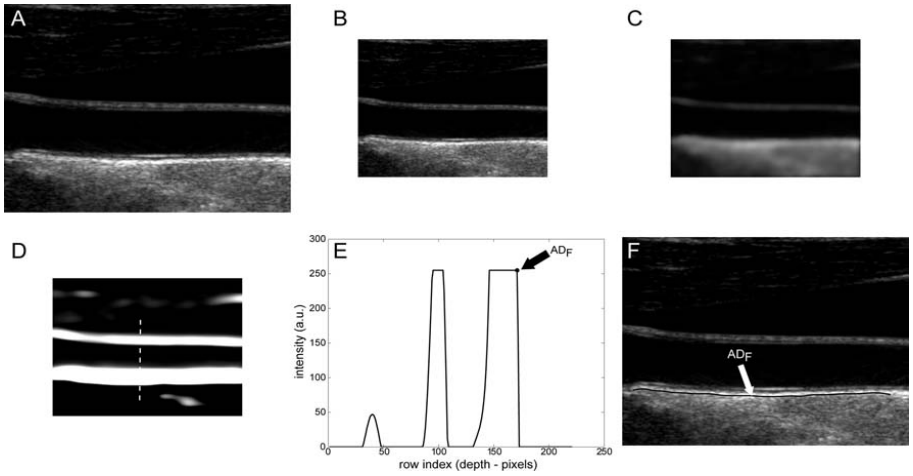

Fig. 1. CADLES-EF procedure for AD_F tracing. **(A)** Original cropped image. **(B)** Downsampled image. **(C)** Despeckled image. **(D)** Image after convolution with first-order Gaussian derivative (sigma = 8). **(E)** Intensity profile of the column indicated by the vertical dashed line in panel D. (AD_F indicates the position of the far adventitia wall). **(F)** Cropped image with far adventitia

specific case of carotid imaging.

- *Step 3*: *Higher order Gaussian derivative filter*. The despeckled image is then filtered using a 35x35 pixels first-order derivative of a Gaussian kernel. The scale parameter of the Gaussian derivative kernel is taken equal to 8 pixels. This value is chosen because it is equal to half the expected dimension of the IMT value in an original fine resolution image, since an average IMT value equal to 1 mm corresponds roughly to about 16 pixels in the original image scale and therefore 8 pixels in the down-sampled image. The white horizontal stripes in Figure 1.D show the proximal (near) and distal (far) adventitia layers.
- *Step 4*: *Automated Far Adventitia (AD_F) tracing*. Figure 1.E shows the intensity profile of one column (from the upper edge of the image to the lower edge of the image) of the Gaussian filtered image. The proximal (near) and distal (far) walls are identifiable as intensity maxima saturated to 255. A heuristic search is used to automatically trace the profile of the distal (far) wall. This search starts from the bottom of the image and searches for the first white region consisting of at least 6 pixels. The deepest point of this region (*i.e.* the pixel with the highest row index) marks the position of the far adventitia AD_F layer on that column. The AD_F profile that is found is then up-sampled to the original scale (Figure 1.F).

B. Stage-II: Edge-Flow model (Strong LI/MA Edgs)

A Guidance Zone is traced starting from the AD_F profile and by extending it 50 pixels above, to comprise the distal wall.

The Edge Flow algorithm, originally proposed by Ma and Manjunath [6], facilitates the integration of different image attributes into a single framework for boundary detection and is based on the construction of an Edge Flow vector $F(s,\theta)$ defined as

$$F(s,\theta) = F[E(s,\theta), P(s,\theta), P(s,\theta+\pi)] \quad (1)$$

where:

- $E(s,\theta)$ is the edge energy at location s along the orientation θ;
- $P(s,\theta)$ represents the probability of finding the image edge boundary if the corresponding Edge Flow "flows" in the direction θ;
- $P(s,\theta+\pi)$ represents the probability of finding the image edge boundary if the Edge Flow "flows" backwards, *i.e.,* in the direction $\theta+\pi$.

Considering the original image *I(x,y)* at a certain scale σ, $I_\sigma(x,y)$ is obtained by smoothing the original image with a Gaussian kernel $G_\sigma(x,y)$. The intensity Edge-Flow energy $E(s,\theta)$ at scale σ, defined to be the magnitude of the gradient of the smoothed image $I_\sigma(x,y)$ along the orientation θ, can be computed as

$$E(s,\theta) = |I(x,y) * GD_{\sigma,\theta}| \quad (2)$$

where s is the location *(x,y)* and $GD_{\sigma,\theta}$ is the first-order Gaussian Derivative along θ. This energy indicates the strength of the intensity changes. To compute $P(s,\theta)$, two possible flow directions (θ and $\theta+\pi$) are considered for each of the edge energies along the orientation θ at location s. The prediction error toward the surrounding neighbors in these two directions can be computed as:

$$\begin{aligned} Error(s,\theta) &= |I_\sigma(x+d\cos\theta, y+d\sin\theta) - I_\sigma(x,y)| \\ &= |I(x,y) * DOOG_{\sigma,\theta}(x,y)| \end{aligned} \quad (3)$$

where d is the distance of the prediction and it should be proportional to the scale at which the image is being analyzed. $DOOG_{\sigma,\theta}(x,y)$ indicates the Difference-of-offset-Gaussian. The probabilities of Edge-Flow direction are then assigned in proportion to their corresponding prediction errors, due to the fact that a large prediction error in a certain direction implies a higher probability of locating a boundary edge in that direction:

$$P(s,\theta) = \frac{Error(s,\theta)}{Error(s,\theta) + Error(s,\theta+\pi)} \quad (4)$$

The texture Edge-Flow can be computed with the same technique as the Intensity Edge-Flow, starting from a Gabor decomposition of the image at the scale σ.

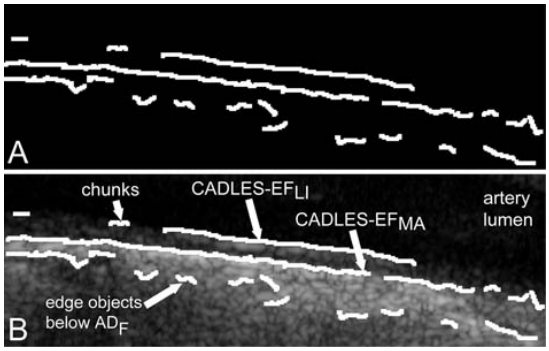

Fig. 2. **(A)** Binary edge output from the Edge Flow algorithm. **(B)** Superposition of the binary edges on the corresponding grayscale carotid Guidance Zone.

Finally, the Edge Flows obtained from the two different types of image attributes can be combined:

$$E(s,\theta)=\sum_{a\in A}E_a(s,\theta)\cdot w(a) \quad , \quad \sum_{a\in A}w(a)=1 \tag{5}$$

$$P(s,\theta)=\sum_{a\in A}P_a(s,\theta)\cdot w(a) \tag{6}$$

where $E_a(s,\theta)$ and $P_a(s,\theta)$ represent the energy and probability of the Edge Flow computed from the image attributes *a* (in our case, intensity and texture). *w(a)* is the weighting coefficient among various types of image attributes.

The vector sum of the Edge Flows with their directions in the identified range is what defines the final resulting Edge Flow and is given by:

$$\vec{F}(s)=\sum_{\Theta(s)\le\theta\le\Theta(s)+\pi}E(s,\theta)\cdot\exp(j\theta) \tag{7}$$

where $\vec{F}(s)$ is a complex number whose magnitude represents the resulting edge energy and whose angle represents the flow direction.

Once the Edge-Flow $\vec{F}(s)$ of an image is computed, boundary detection can be performed by iteratively propagating the Edge-Flow and identifying the locations where two opposite direction of flows encounter each other. The local Edge-Flow is then transmitted to its neighbor in the direction of flow if the neighbor also has a similar flow direction. Fig. 2.A shows an example of an output image from the Edge Flow algorithm, whereas fig. 2.B shows this output binary image overlaid on the original image. Clearly, Edge-Flow over-segments the image.

C. MA Edge refinement by Labeling/Connectivity

Three main challenges must be faced in presence of over-segmentation (see fig. 2.B):

1. removing the incorrect edge objects outside the region of interest;
2. removing the small edge objects in the region of interest;
3. connecting chunks edge objects.

The solution to challenge (1) is simply the deletion of all the edge objects in the output image that are not included in the Guidance Zone.

The solution to challenge (2) requires the definition of a small edge object. Small edge objects around the ROI are defined as those that have an area ratio below a limit ϕ when compared to the totality of the edge objects of the image. The area ratio is defined by the following equation:

$$AreaRatio=\frac{Area_{EdgeObject}}{Area_{AllEdgeObjects}}\le\phi\Rightarrow SmallEdgeObject \tag{8}$$

Our experimental data showed that ϕ=*0.1* is an optimal value to guarantee the rejection of the small edge objects.

The solution to challenge (3) is based on the identification of those chunks, which can be linked to form the final MA edge object. The MA segment is first initialized as being the edge object with the highest pixel row index. The remaining small edge objects are scanned one by one and are assigned to the MA edge object if they are located on the MA boundary (intensity check) and close and aligned to the MA edge object (geometrical check).

D. LI Edge refinement using MA constraints

The post-processing of the LI edge is more complicated with respect to that of MA. Beside the problem of over-segmentation (*i.e.*, of the LI profile broken into chunks), there is the problem of false edge objects located in the vessel lumen (*i.e.*, above LI) and in the media layer (*i.e.*, in between MA and LI). This is mainly due to blood backscattering in the CA lumen.

Each LI object is validated through a heuristic procedure that rejects edge objects made of too dark pixels (since possibly located in the CA lumen) and of too bright pixels (since possibly located in the media layer).

Then each LI edge object is compared to the MA profile: all the edge objects that are closer than 0.3 mm and farther than 1.5 mm are discarded (the values have been derived by considering the standard IMT value of 0.8 mm). The remaining edge objects are connected to form the final LI boundary.

Fig. 3 shows samples of CADLES-EF segmentation.

III. Results and Discussion

We tested CADLES-EF on a 300 images database, which is multi-institutional, multi-ethnic, multi-scanner, and multi-operator. One-hundred images were acquired at Cyprus Institute of Neurology and Genetics (Nicosia, Cyprus), 200 were acquired at the Neurology Division of the Gradenigo Hospital (Torino, Italy). Pixel density was equal to 16.67 px/mm and 16 px/mm for Cyprus and Italy images, respectively. Demographics of the patients can be found in previous works [5, 7].

CADLES-EF correctly identified the carotid artery by tracing of the AD_F profile in all 300 images (100% success rate). The average distance between CADLES-EF_{LI} tracings and GT_{LI} tracings was 0.475±1.660 mm, which of the MA profiles was 0.176±0.202 mm. The average IMT measurement bias was equal to 0.043±0.189 mm, with a tendency towards overestimation of IMT (see Table I). The Figure-of-Merit was equal to 94.8%.

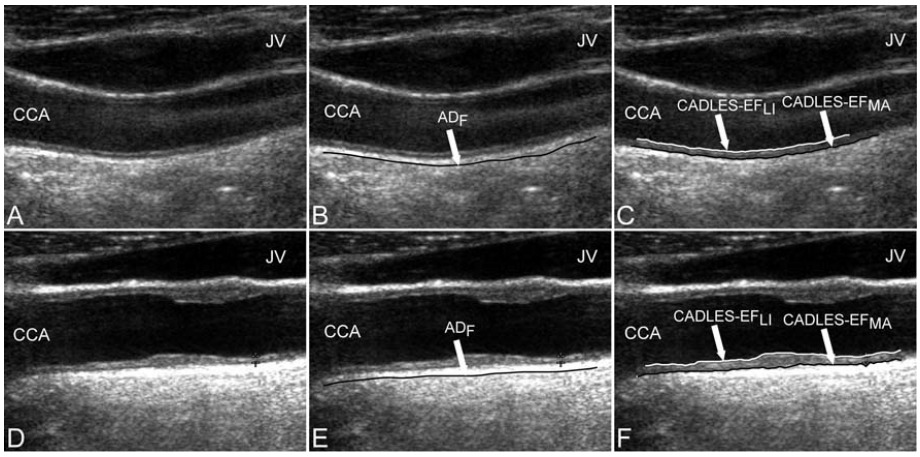

Fig. 3. Examples of CADLES-EF performance on normal but non-horizontal carotid artery and carotid artery in the presence of jugular vein. **First Column**: the original cropped images; **Middle Column**: AD_F profile (stage-I output) overlaid on the original cropped grayscale images; Last **Column**: LI and MA borders estimated using CADLES-EF algorithm overlaid on the original grayscale images.

CADLES-EF was compared to two previously developed automated techniques called CALEXia [7, 8] and CULEXsa [7, 9]. The overall FoM for CALEXia was found to be equal to 84.7%, while for CULEXsa it was equal to 91.5%. We found that CALEXia underestimates the IMT, while CULEXsa tends to underestimate the IMT value in a manner more similar to CADLES-EF (even though with slightly more marked tendency towards underestimation).

The major advantage of this new technique is versatility: unlike CULEXsa, the most performing benchmarking technique, CADLES-EF always reached convergence. Being based on snakes, CULEXsa showed convergence issues when in presence of small plaques or of deformed vessels, due to the difficulty of fine-tuning the snake tension and elasticity. As a result, CULEXsa could not process 14 images out of 300. CADLES-EF offered satisfactory LI/MA segmentation performance and proved effective in following any vessel morphology, without changing any system parameters, unlike CULEXsa. Compared to CALEXia, CADLES is more robust with respect to image noise.

The computational time was comparable. Using MATLAB on a dual 2.5 GHz PC equipped by 8 MB of RAM, CADLES-EF took 60 s compared to 50 s for CULEX. CALEXia was the fastest at 3 s.

TABLE I – COMPUTER ESTIMATED IMT AND GROUND-TRUTH IMT FOR THE THREE TECHNIQUES. LAST COLUMN IS FIGURE-OF-MERIT.

	Estimated IMT (mm)	GT IMT (mm)	FoM
CADLES-EF	0.861±0.276	0.818±0.246	94.8 %
CALEXia	0.746±0.156	0.880±0.164	84.7%
CULEXsa	0.805±0.248	0.879±0.237	91.5 %

IV. CONCLUSION AND FUTURE PERSPECTIVES

The CADLES-EF algorithm we developed can be proficiently used for the segmentation of B-mode longitudinal ultrasound images of the carotid wall. It is completely user-independent: the raw US image can be completely processed without any interaction with the operator. It is based on a scale-space multi-resolution analysis to determine initial location of the carotid artery in the image and then using the flow field propagation based on intensity and texture to determine strong edges, which are then classified and refined to provide the final contours of the LI and MA interfaces.

From a clinical point of view, the algorithm traces the boundaries of both the intima and media layers, which can be used for measurements. We are currently developing a multi-institutional database for a comprehensive study to validate the clinical applicability of our work.

REFERENCES

[1] F. Molinari, G. Zeng, and J. S. Suri, "A state of the art review on intima-media thickness (IMT) measurement and wall segmentation techniques for carotid ultrasound," *Computer Methods and Programs in Biomedicine*, 2010 (in press).

[2] A. C. Rossi, P. J. Brands, and A. P. Hoeks, "Automatic recognition of the common carotid artery in longitudinal ultrasound B-mode scans," *Med Image Anal,* vol. 12, no. 6, pp. 653-65, Dec, 2008.

[3] S. Golemati, J. Stoitsis, E. G. Sifakis *et al.*, "Using the Hough transform to segment ultrasound images of longitudinal and transverse sections of the carotid artery," *Ultrasound Med Biol,* vol. 33, no. 12, pp. 1918-32, Dec, 2007.

[4] R. Rocha, A. Campilho, J. Silva *et al.*, "Segmentation of the carotid intima-media region in B-Mode ultrasound images," *Image and Vision Computing,* vol. 28, no. 4, pp. 614-625, 2010.

[5] C. P. Loizou, C. S. Pattichis, C. I. Christodoulou *et al.*, "Comparative evaluation of despeckle filtering in ultrasound imaging of the carotid artery," *Ultrasonics, Ferroelectrics and Frequency Control, IEEE Transactions on,* vol. 52, no. 10, pp. 1653-1669, 2005.

[6] W. Y. Ma, and B. S. Manjunath, "Edge Flow: A Framework of Boundary Detection and Image Segmentation." pp. 744-749.

[7] F. Molinari, G. Zeng, and J. S. Suri, "Intima-media thickness: setting a standard for completely automated method for ultrasound," *IEEE Transaction on Ultrasonics Ferroelectrics and Frequency Control,* vol. 57, no. 5, pp. 1112-1124, 2010.

[8] F. Molinari, G. Zeng, and J. S. Suri, "An integrated approach to computer- based automated tracing and its validation for 200 common carotid arterial wall ultrasound images: A new technique," *J Ultras Med,* vol. 29, pp. 399-418, 2010.

[9] S. Delsanto, F. Molinari, P. Giustetto *et al.*, "Characterization of a Completely User-Independent Algorithm for Carotid Artery Segmentation in 2-D Ultrasound Images," *Instrumentation and Measurement, IEEE Transactions on,* vol. 56, no. 4, pp. 1265-1274, 2007.